



HAL
open science

Modelling of the packet delivery rate in an actual LoRaWAN network

Ahmed Abdelghany, Bernard Uguen, Christophe Moy, Dominique Lemur

► **To cite this version:**

Ahmed Abdelghany, Bernard Uguen, Christophe Moy, Dominique Lemur. Modelling of the packet delivery rate in an actual LoRaWAN network. *Electronics Letters*, 2021, 57 (11), pp.460-462. 10.1049/ell2.12165 . hal-03244861

HAL Id: hal-03244861

<https://hal.science/hal-03244861>

Submitted on 5 Jun 2023

HAL is a multi-disciplinary open access archive for the deposit and dissemination of scientific research documents, whether they are published or not. The documents may come from teaching and research institutions in France or abroad, or from public or private research centers.

L'archive ouverte pluridisciplinaire **HAL**, est destinée au dépôt et à la diffusion de documents scientifiques de niveau recherche, publiés ou non, émanant des établissements d'enseignement et de recherche français ou étrangers, des laboratoires publics ou privés.



Distributed under a Creative Commons Attribution 4.0 International License

Electronics Letters

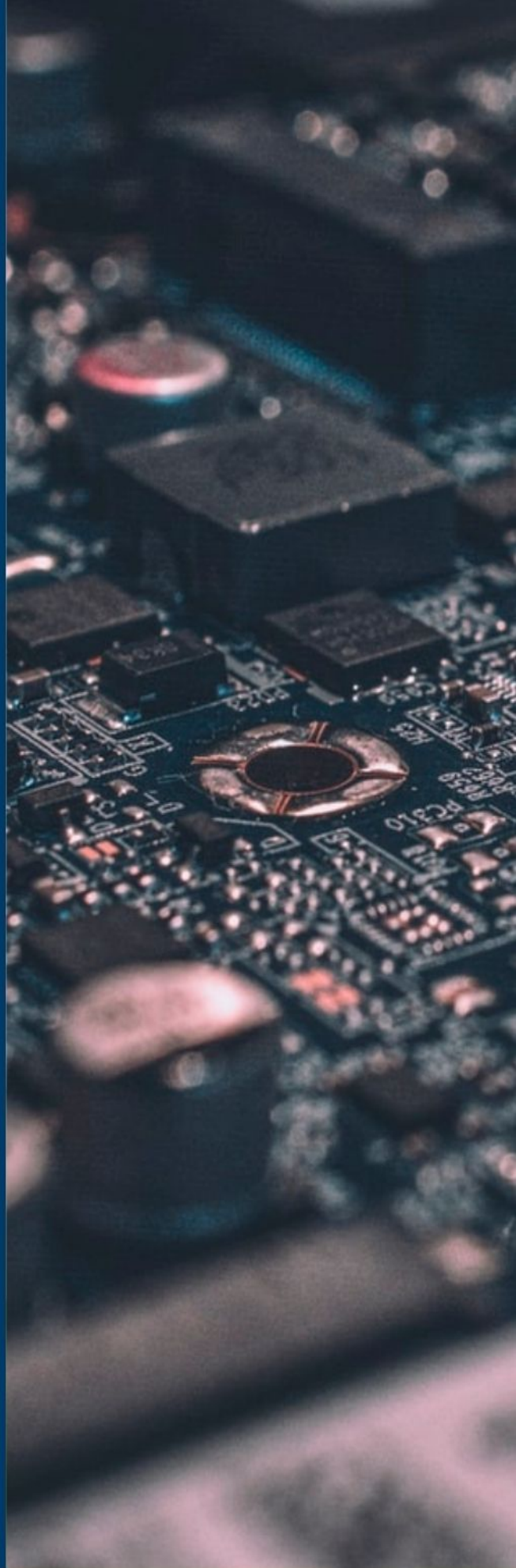
Special issue Call for Papers

**Be Seen. Be Cited.
Submit your work to a new
IET special issue**

Connect with researchers and experts in your field and share knowledge.

Be part of the latest research trends, faster.

[Read more](#)



The Institution of
Engineering and Technology

Modelling of the packet delivery rate in an actual LoRaWAN network

Ahmed Abdelghany,  Bernard Uguen, Christophe Moy,  and Dominique Lemur
Univ Rennes, CNRS, IETR - UMR 6164, Rennes, France
 Email: ahmed.abdelghany@univ-rennes1.fr

The Internet of things (IoT) paradigm is paving the way to ensure connectivity and monitoring within different market fields. Thus, it is critical to understand the packet transmission performance in Low Power Wide Area Network (LPWAN), especially LoRaWAN. Packet delivery rate (PDR) is considered as a dominant factor of the network performance and its dependency on the signal power. However, previous works do not model the PDR as a function of the received signal power. An in-depth investigation of the PDR is done by performing an outdoor measurement campaign in the area of the Campus Beaulieu in Rennes. For each received LoRa packet, the effective signal power (ESP) values are obtained as well as their high influence on PDR is proven. With the given results, modelling the PDR using an ESP-parameterized beta distribution function is proposed. Feasibility of the proposed model is assured by simulating PDR against ESP, hence, the simulated PDR values follow the distribution of the measured ones well. This PDR model gives important guidelines for future LoRaWAN network regulation and optimization.

Introduction: Internet of things (IoT) has been employed in a wide range of domains, such as healthcare, public safety, environmental monitoring, and household [1]. This plethora of IoT applications requires a large coverage network, low power consumption, as well as a cheap deployment. This requirement is difficult to be achieved using the traditional cellular or the short-range wireless networks, hence, Low Power Wide Area Network (LPWAN) is considered the major technology for providing this connectivity, particularly the LoRaWAN. This ability is manifested in the LoRaWAN's design which is based on chirp spread spectrum (CSS) with integrated forward error correction (FEC), thus, it significantly improves the sensitivity of the receiver and makes it robust to interference. Accordingly, the typical LoRa devices can compromise between low energy consumption with their long battery lifetimes at the scale of up to several years, while covering distances of more than 10 km in the unlicensed industrial, scientific and medical (ISM) spectrum [2].

LoRa Alliance standardizes LoRaWAN network protocol at the MAC layer [3], while LoRa modulation, that is, patented by Semtech Corporation, is utilized at the physical layer. The performance of this long-range star network is affected by the rate of data packet loss [4]. Thus, the packet loss between the end node and the gateway degrades the reliability of connections in the network. This transmission failure may occur due to the channel preemption or attenuation; consequently, it is affecting various IoT applications and even causes serious problems. Additionally, a large amount of packet loss may reduce the data integrity and accuracy in IoT data analytics. Therefore, both unconfirmed and confirmed, that is, most probably used for important sensor data, messages are offered by LoRaWAN. Only when sending a confirmed message, the end node requires the message to be acknowledged as received by the network server. Consequently, the end node will retransmit the data packet when it does not receive the acknowledgement. However, this retransmission increases the power consumption of end node devices in addition to occupying an additional spectrum, leading to overwhelming contention and interference on the common spectrum resources.

Recently, the different origins of LoRa packet loss are mentioned in many papers. For example, in [5] experiments are conducted to evaluate a characterization of LoRaWAN frame collision conditions. On the other hand, the packet delivery rate (PDR) and coverage of LoRa technology are evaluated for outdoor cases in [6–8]. Based on studies on the impact of environmental factors on the performance of LoRa in [9], authors show that higher temperatures decrease the Received Signal Strength Indicator (RSSI) and evidently affect PDR. While the first attempt to investigate the PDR in a real city-scale LoRaWAN network is

Table 1. LoRaWAN configuration

LoRaWAN parameter	Value
Modulation technique	LoRa (based on CSS)
Spreading factor (SF)	7
Coding rate	4/5
Bandwidth W	125 kHz
Transmit power	14 dBm
Centre frequency f_k	{867.1, 867.3, 867.5, 867.7, 867.9, 868.1, 868.3, 868.5} MHz



FIGURE 1 The gateway connected to the antenna cable

presented in [10]. However, these previous works do not introduce the modelling of PDR corresponding to the received power. Hence, the received power is considered as one of the main factors affecting the PDR.

An in-depth investigation of the PDR is done using the traces collected from a real network deployment in the area of the Campus Beaulieu in Rennes. Hence, the whole effective signal power (ESP), that is introduced in [11], values in the experiment are extensively evaluated, and a stochastic model is proposed for modelling PDR as a function of the ESP rather than using RSSI to overcome the RSSI's limitation, especially at low signal-to-noise ratio (SNR) (< 0 dB).

Measurement setup: The main target of the proposed experiment is obtaining the ESP against the PDR for each channel. This is done by setting the LoRaWAN configuration as presented in Table 1. Thus, confirmed LoRa packets are transmitted sequentially at the typical frequency bands for Europe, that is, eight channels with centre frequency f_k . A Tektelic KONA Macro Gateway is used whose antenna is fixed on the roof of the university building [13], as shown in Figure 1. While an IoT node is placed at various locations, hence, the distance between the gateway and the node gradually increases from ≈ 5 m to ≈ 760 m. This end node is implemented using a Pycom card that is programmed in the MicroPython language, composed of an Expansion Board and an LoPy 4 module which can support LoRa wireless connectivity [12], as shown in Figure 2.

For each specific channel f_k , the Pycom node transmits an uplink packet. While the gateway attempts to send an acknowledgement by default at the same frequency as the message transmitted. Accordingly, the node writes the information of the last received downlink packet (packet number, ESP, etc.) to the payload of the next uplink packet. For this experiment, a desktop computer runs a Python program and is used as an Application Server (AS) which receives data from the LoRa Network Server (LNS), as well as LoRa metadata with all parameters of the LoRaWAN transmission (f_k , spreading factor (SF), bandwidth W , RSSI, SNR, etc.). Thus, the computer stores this data for processing as detailed in the following sections, moreover, the data is provided to the research society on this online repository [14].



FIGURE 2 The packaged Pycom device fixed on a rod and connected to a battery

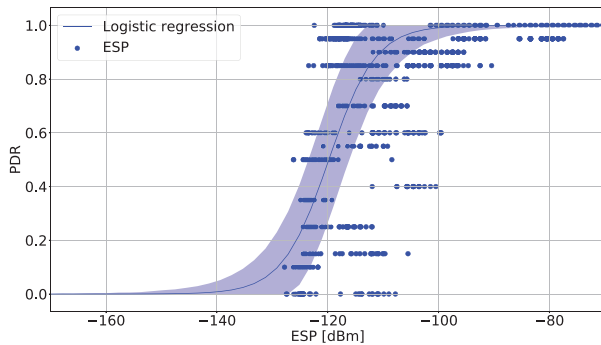


FIGURE 3 Measured PDR versus different ESP values

Measurement results: In an offline mode, the received data is extracted from the payload of each LoRa packet at the gateway side. ESP is proven in [11] to have an enlarged range unlike the RSSI which has a limitation when the SNR is very low (< 0 dB). Therefore, ESP value is extracted and analyzed against the PDR value at each frequency channel f_k . Without lack of generality, ESP is computed as:

$$ESP_{\text{dBm}} = RSSI_{\text{dBm}} + SNR_{\text{dB}} - 10 \log_{10}(1 + 10^{0.1SNR_{\text{dB}}}). \quad (1)$$

On the other hand, PDR is calculated at each different channel f_k independently as:

$$PDR = \frac{\text{Number of received packets}}{\text{Number of transmitted packets}}, \quad (2)$$

where the number of transmitted packets to obtain the PDR value at each frequency band f_k is 20. Figure 3 explores how PDR changes along with ESP. The result shows that high PDR values reduce significantly with the decrease of ESP. Therefore, ESP has a simpler and more natural relationship with PDR than RSSI. Moreover, one can observe that the PDR magnitudes are uniformly quantized with a resolution of $\frac{1}{20}$. Nevertheless, there are some irregular gaps between the PDR values, which could be compensated by taking more measurement data.

Pdr modelling: For system-level simulations or for dimensioning actual IoT deployment performances, it is very useful to benefit from a PDR model that encompasses all the possible situations and their very large observed variability. However, the PDR values show extreme variations which make the exploitation of their empirical mean difficult. Therefore, the first step of the proposed approach is to get access to a reasonable estimation of the expected PDR average by logistic regression. This regression takes into account all the datasets at once by fitting a smooth and reasonable curve to the measured values. Consequently, the mean of the PDR distribution can have a deterministic model using a logistic function or logistic curve which is a common sigmoid curve with an equation as:

$$\mathbb{E}[PDR] = \frac{1}{1 + e^{-k(ESP - ESP_0)}}, \quad (3)$$

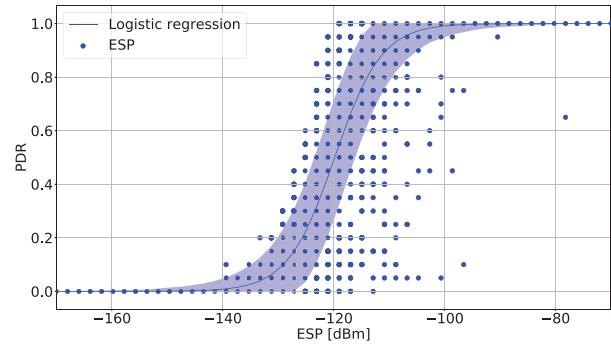


FIGURE 4 Simulated PDR versus different ESP values

where k is the logistic growth rate or steepness of the curve which is estimated to be 0.238. While the ESP value of the sigmoid's midpoint ESP_0 is -119.794 dBm. These parameters are estimated while setting SF equal to 7 during the experiment, hence, these values can be different if another configuration is set. On the other hand, the expected PDR values lie around an interval that can be sized with a given level of confidence 2σ . This σ value is obtained based on the number of packets used in this experiment to produce the empirical estimation of each PDR value. This confidence region is the shaded blue region in Figure 3, accordingly, the PDR values are estimated roughly around this region.

In a second step, in order to simulate the observed huge variability in the measured PDR, an ESP parameterized Beta distribution of PDR is proposed [15]. Consequently, the probability density function (pdf) of the PDR distribution can have a stochastic model using a Beta distribution function as:

$$f(PDR; \alpha, \beta) = \frac{1}{B(\alpha, \beta)} PDR^{\alpha-1} (1 - PDR)^{\beta-1} \quad (4)$$

$$= \frac{\Gamma(\alpha + \beta)}{\Gamma(\alpha)\Gamma(\beta)} PDR^{\alpha-1} (1 - PDR)^{\beta-1}$$

with

$$\Gamma(z) = \int_0^{\infty} x^{z-1} e^{-x} dx, \quad (5)$$

where $\Gamma(z)$ is the gamma function. While the beta function $B(\alpha, \beta)$ is a normalization constant to ensure that the total probability is 1. In the above equation, PDR is a realization, that is, an estimated PDR value that actually occurred, of a random process. Moreover, this Beta distribution function $f(PDR; \alpha, \beta)$ has a mean $\mathbb{E}[PDR]$ which is computed as:

$$\mathbb{E}[PDR] = \frac{\alpha}{\alpha + \beta}. \quad (6)$$

By exploiting the noticeable formal similarity between the two expressions of the expectation in Equations (3) and (6), α and β are estimated as $\alpha = 1$ and $\beta = e^{-k(ESP - ESP_0)}$. At this point, these can also be redefined as:

$$\mathbb{E}[PDR] = \frac{1}{1 + \beta} \quad (7)$$

and the variance $\text{Var}[PDR]$ is:

$$\text{Var}[PDR] = \frac{\alpha\beta}{(\alpha + \beta)^2(\alpha + \beta + 1)} = \frac{\beta}{(1 + \beta)^2(\beta + 2)}. \quad (8)$$

Simulation results: In this section, the performance of the proposed PDR model is evaluated by generating PDR distributions at each ESP value. Figure 4 shows the simulated PDR distribution which follows the distribution of the measured PDR in Figure 3. Consequently, the expectation of the simulated PDR values lies within the 2σ confidence interval around the sigmoid curve, whereas the extreme variations of the PDR are well simulated as promised by this proposed model. For obtaining the same resolution of the measured PDR, the simulated PDR values are uniformly quantized with the same resolution of the measured PDR.

On the other hand, the PDR distribution is different at each ESP value as manifested by their corresponding Beta distribution functions in Figure 5. For example, the Beta distribution function at -130 dBm has a distribution concentrated around low PDR values, in contradiction with the distribution at -110 dBm which has high PDR values. While the

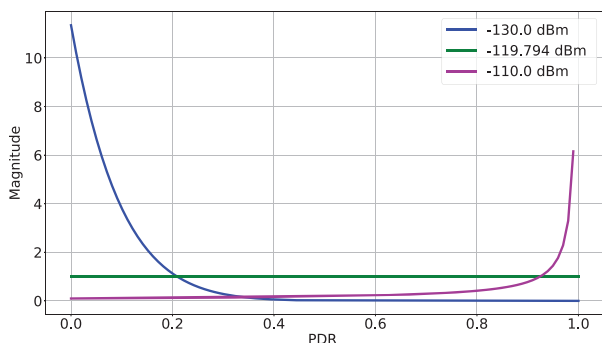


FIGURE 5 Beta distribution function $f(PDR; \alpha, \beta)$ at different ESP values

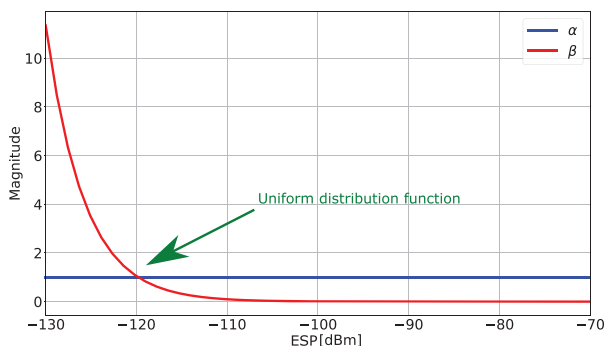


FIGURE 6 α and β evolution against ESP

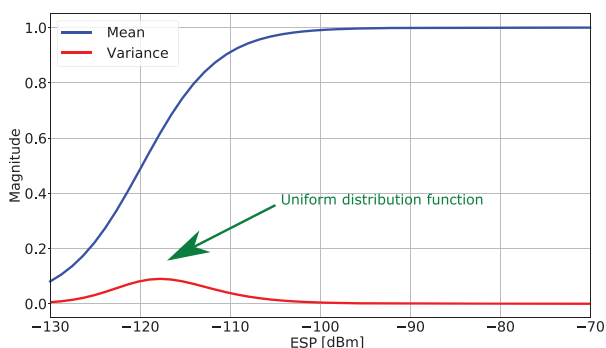


FIGURE 7 Mean $\mathbb{E}[PDR]$ and variance $Var[PDR]$ evolution against ESP

distribution at -119.794 dBm, that is, sigmoid's midpoint ESP_0 as depicted in Equation (3), is considered the most ambiguous one which is an almost uniform distribution. In this uniform case, the PDR has an equivalent probability of success and failure.

Moving to the fine parameters of the Beta distribution function $f(PDR; \alpha, \beta)$, Figure 6 shows the constant α and the variable β across different ESP values. One can observe that as β is changed, the shape of the distribution changes. As α becomes larger than β (more successful packets), the bulk of the probability distribution will shift towards the high PDR values as shown in Figure 4, whereas an increase in β moves the distribution towards the low PDR values (more failures). While α and β are equal to 1 at -119.794 dBm which is depicted by a green arrow and as a uniform distribution function in Figure 4.

Focusing on the introduced mean $\mathbb{E}[PDR]$ and variance $Var[PDR]$ of the Beta distribution function, Figure 7 showcases their values with a wide range of ESP values. Generally, as ESP increases, the mean increases until it starts to saturate when ESP is above -100 dBm. While the variance is very small at most of the ESP values, however, it has a peak when the ESP is around -119.794 dBm as shown by the green arrow. This peaky region is indicated in Figure 4 when PDR distribution has a large variance around -119.794 dBm.

Conclusion: ESP is considered to be more reliable than RSSI as it overcomes the RSSI limitation, especially at low SNR (< 0 dB). Accordingly, this paper presents the modelling of the PDR as a function of ESP. Thus, a measurement campaign is carried out in the city of Rennes to estimate the channel ESP from different node locations. Hence, the

measured PDR is investigated against ESP and is modelled using a Beta distribution function. Besides, the PDR distribution is simulated using the proposed model, as a result, the simulated PDR follows the measured one well. Furthermore, the fine parameters of the Beta distribution function are tuned at each ESP value for analysing their effect on the PDR distribution.

For future work, this paper recommends using this Beta distribution function for modelling PDR as a function of ESP. Thus, the potential studies in IoT can simulate the PDR against ESP to have an estimation for dimensioning the LoRaWAN network.

Acknowledgement: We are grateful to Jean Franois Legendre from Gwagenn Company for borrowing us the gateway [16].

© 2021 The Authors. *Electronics Letters* published by John Wiley & Sons Ltd on behalf of The Institution of Engineering and Technology

This is an open access article under the terms of the Creative Commons Attribution License, which permits use, distribution and reproduction in any medium, provided the original work is properly cited.

Received: 12 February 2021 Accepted: 17 March 2021

doi: 10.1049/ell2.12165

References

- Ghany, A.A., Uguen, B., Lemur, D.: A pre-processing algorithm utilizing a paired CRLB for TDMA based IoT positioning. In: 2020 IEEE 91st Vehicular Technology Conference (VTC2020-Spring), pp. 1–5, Antwerp, Belgium (2020) <https://doi.org/10.1109/VTC2020-Spring48590.2020.9128385>
- Oliveira, R., Guardalben, L., Sargento, S.: Long range communications in urban and rural environments. In: 2017 IEEE Symposium on Computers and Communications (ISCC), pp. 810–817, Heraklion (2017) <https://doi.org/10.1109/ISCC.2017.8024627>
- LoRa-Alliance - Retrieved February 15, 2021, from <https://www.lora-alliance.org/>
- Augustin, A., et al.: A study of LoRa: Long range & low power networks for the internet of things. *Sensors* **16**, 1466 (2016)
- Rahmadhani, A., Kuipers, F.: When LoRaWAN frames collide. In: Proceedings of the 12th International Workshop on Wireless Network Testbeds, Experimental Evaluation & Characterization (WiNTECH '18), pp. 89–97. Association for Computing Machinery, New York, NY, USA (2018). <https://doi.org/10.1145/3267204.3267212>
- Li, L., Ren, J., Zhu, Q.: On the application of LoRa LPWAN technology in sailing monitoring system. In: 2017 13th Annual Conference on Wireless On-demand Network Systems and Services (WONS), pp. 77–80, Jackson, WY, USA (2017) <https://doi.org/10.1109/WONS.2017.7888762>
- Wang, S. et al.: Performance of LoRa-based IoT applications on campus. In: 2017 IEEE 86th Vehicular Technology Conference (VTC-Fall), pp. 1–6, Toronto, ON (2017) <https://doi.org/10.1109/VTCFall.2017.8288154>
- Seye, M.R. et al.: A study of LoRa coverage: Range evaluation and channel attenuation model. In: 2018 1st International Conference on Smart Cities and Communities (SCCIC), pp. 1–4, Ouagadougou, (2018) <https://doi.org/10.1109/SCCIC.2018.8584548>
- Cattani, M., Boano, C.A., R mer, K.: An experimental evaluation of the reliability of LoRa long-range low-power wireless communication. *J. Sens. Actuator Netw.* **6**, 7 (2017)
- Liu, Q. et al.: Characterizing packet loss in city-scale LoRaWAN deployment: Analysis and implications. In: 2020 IFIP Networking Conference (Networking), pp. 704–712, Paris, France (2020)
- Rahmadhani, A., Kuipers, F.: Understanding collisions in a LoRaWAN. (2017). Project: Iot - surfnet-network home. (n.d.). Retrieved February 15, 2021, from <https://wiki.surfnet.nl/display/SURFnetnetwerkWiki/Project%3A+IoT?preview=%2F11211020%2F11211313%2FTUD-LoRaWAN-RoN-2017.pdf>
- Pycom documentation: <https://GitHub.com/PyCom/PyCom-libraries>.
- Tektelic KONA Macro IoT Gateway. <https://www.tektelic.com/uploads/Brochures/Kona%20Macro.pdf>
- Measurement Data. <https://gitlab.com/ahmednagy/lorawan-beaulieu-measurement-2020>
- Kerman, J.: A closed-form approximation for the median of the beta distribution. (2011). arXiv: Statistics Theory.
- Gwagenn company website. <http://www.gwagenn.com/en/home/>